# SENSITIVITY STUDY ON A CFD MODEL FOR THE ANALYSIS OF MODERATOR FLUID FLOW AND HEAT TRANSFER INSIDE CANDU CALANDRIA

G. H. Lee<sup>1</sup> and S. W. Woo<sup>1</sup>

<sup>1</sup> Korea Institute of Nuclear Safety, Daejon, Republic of Korea <a href="mailto:ghlee@kins.re.kr">ghlee@kins.re.kr</a>, <a href="mailto:k097wsw@kins.re.kr">k097wsw@kins.re.kr</a>

#### Abstract

In this paper, sensitivity study on a CFD model for the accurate analysis of moderator fluid flow and heat transfer inside calandria is conducted. Two main items, i.e. porous medium assumption and turbulence model, are considered for in-line tube bank [1] and Sheridan Park Engineering Laboratory (SPEL) experiment [2]. Using the commercial flow solver, FLUENT [3], the prediction to consider the real geometry of fuel channels is compared to previous results conducted with the porous medium assumption using the isotropic pressure loss model. Also, the prediction performance of various turbulence models (e.g. k-ε model, Reynolds stress model, etc.) is assessed.

#### 1. Introduction

The prevention of calandria tube dryout resulting from the contact between pressure tube and calandria tube depends on available local moderator subcooling. To estimate the local subcooling of the moderator inside CANDU calandria under normal operational condition or transient conditions (for example, loss of coolant accident (LOCA) with the coincident failure of the emergency coolant injection system) is one of the major concerns in the CANDU safety analysis. In view of the severe consequences of fuel channel failures, and the small safety margins that currently exist with respect to moderator temperature (or moderator subcooling) requirements, the Canadian Nuclear Safety Commission (CNSC) staff categorized the moderator temperature prediction as a generic action item (No. 95G05) and requested the validation of the computer code used to calculate the moderator temperature distribution against three-dimensional moderator tests [4].

Extensive CFD analyses have been performed for predicting the moderator temperature in a CANDU reactor or its similar shape. Collins [5] numerically solved two distinct flow patterns, that is, momentum dominated and buoyancy dominated flow pattern, inside the SPEL experimental facility and compared the prediction with the experimental data. Huget et al. [6] validated the CFD code, MODTURC\_CLAS, against the Moderator Test Facility (MTF) experimental data representing a range of CANDU 9 reactor conditions. They obtained relatively good quantitative agreement between the code prediction and measurements of three-dimensional moderator temperature distribution in the MTF vessel at Chalk River Laboratories.

Although several analyses were performed with three-dimensional CFD codes, the porous medium assumption was used instead of considering the real geometry of calandria tube installed in the vessel. For example, Yoon and Park [7] developed the moderator analysis model based on the ANSYS CFX code together with a porous medium assumption for the core region in order to

predict the steady state moderator circulation under operating conditions and the local moderator subcooling during LOCA transients. However, the secondary flow and vortex shedding, which may play an important role in the moderator flow and heat transfer characteristics, cannot be considered in a porous medium assumption. Therefore, it may be necessary to establish the analyses model which can simulate the flow patterns and the temperature distributions reasonably inside calandria vessel by allowing for the real geometry of fuel channels.

To model the turbulence generation and dissipation inside calandria, most of previous studies used the standard k-ε turbulence model with the wall function approach [5,6,7]. However, the appropriateness of this turbulence model to analyse the spreading and interaction of the three-dimensional wall jets emitted by the inlet nozzles is still questioned. Another limitation of the k-ε turbulence model is that it has been formulated and verified primarily in high Reynolds number fully-turbulent flows. If there are large regions of relatively low speed and highly stable zones of hot water inside calandria, the k-ε model may be unsuitable in this case [8].

The main objective of the present study is to investigate whether the porous medium assumption can give the conservative subcooling margin compared to the prediction with real calandria tube geometry and to assess the prediction performance of various turbulence models for the reasonable analysis of moderator flow and heat transfer inside calandria.

The above two main items, i.e. porous medium assumption and turbulence model, are considered for in-line tube bank [1] and SPEL experiment [2]. Using the commercial flow solver, FLUENT [3], the prediction to consider the real geometry of fuel channels is compared to previous results conducted with the porous assumption using the isotropic pressure loss model. Also, the prediction performance of various turbulence models (e.g. k- $\epsilon$  model, Reynolds stress model, etc.) is assessed.

#### 2. Porous medium assumption

A CANDU-6 reactor has 380 fuel channels inside the calandria vessel that extend from one end shield to the other. These fuel channels may be modelled using the concept of isotropic porosity, defined as the average ratio of fluid volume to total volume.

Although the porosity of a CANDU-6 reactor, 0.83, is high enough to allow a porous medium assumption to be used, this assumption has at least three possible weaknesses [6]. First, although the momentum loss term can account for the pressure loss in the mean-flow equations, the increased production of turbulence due to vortex shedding in the wake of the individual tubes is not considered in the turbulence model. Second, it is difficult to identify the true effects of the outer ring of calandria tubes on the generation of the highly non-uniform flows in the reflector region. Although this approach assumes that the outermost tubes exert a volume averaged effect on the local flows, it is questioned for this method to adequately account for the true effects. Third, it is not clear how well the momentum loss models quantitatively represent the three-dimensional effects of the turbulent flows through the calandria tubes. It is difficult to establish a generally applicable form of the empirical pressure drop coefficient. In this section, one of the momentum loss models [9] is briefly explained.

Hydraulic resistance consists of form drag and friction drag. If hydraulic resistance does not depend on the angle of attack between the flow direction and tube axis, the moderator flow can be decomposed into the axial flow and the lateral flow.

For the axial flow, there is no form drag. If the fluid velocity can be decomposed into the x, y, and z components, the hydraulic resistance of the axial flow is able to be expressed by the conventional correlations of frictional pressure loss in a cylindrical pipe.

$$\frac{\Delta P}{\Delta L} \bigg|_{z} = \frac{\Delta P_{fric}}{\Delta Z} = \frac{f \rho u_{z}^{2}}{2D_{e}} \tag{1}$$

where  $\Delta P_{fric}$  is frictional pressure loss,  $\Delta Z$  is axial unit length, f is friction factor,  $\rho$  is density,  $U_z$  is axial component of velocity, and  $D_e$  is hydraulic diameter of axial flow passage.

Friction factor, f, is calculated from the correlation for the flow inside the circular pipes. For the turbulent flow of a low Reynolds number,

$$f = 0.316 \,\mathrm{Re}^{-0.25} \tag{2}$$

Here, Re is the Reynolds number  $\left(=U_zD_e/v\right)$  and v is kinematic viscosity.

For the transverse (lateral) flow across the tube bank, Hadaller et al. [1] investigated the pressure drop of the fluid flows crossing the staggered and in-line tube bank, where the Reynolds number range was 2,000 to 9,000 and the pitch to tube diameter ratio (p/d) was 2.16. They concluded that for the given pitch to tube diameter ratio, the effect of the staggering is not significant. From the experimental investigation, the empirical correlation for the pressure loss coefficient was obtained as

$$PLC \equiv \frac{\Delta P}{N_r \rho V_m^2 / 2} = 4.54 \,\text{Re}^{-0.172}$$
 (3)

where,  $\Delta P$  is the pressure drop,  $N_r$  is the number of tube rows, and  $V_m$  is the free-stream velocity before obstruction.

The hydraulic resistance source term in the momentum equations is in the form of a pressure drop per unit length.

$$\frac{\Delta P}{\Delta L} = 4.54 \,\text{Re}^{-0.172} \,\frac{N_r}{\Delta L} \frac{\rho V_m^2}{2} \tag{4}$$

Note that  $V_m$  is different from the local moderator velocity in the core region of the CANDU calandria vessel,  $V_c$ .

Area porosity can be defined as

$$V_m = \gamma_A V_C \tag{5}$$

Decomposition of the pressure gradient per unit travel length gives

$$\frac{\Delta P}{\Delta L}\Big|_{x} = \frac{\Delta P}{\Delta L} \cos \theta = \frac{\Delta P}{\Delta L} \frac{U_{x}}{V_{c}} \tag{6}$$

$$\frac{\Delta P}{\Delta L}\Big|_{y} = \frac{\Delta P}{\Delta L} \sin \theta = \frac{\Delta P}{\Delta L} \frac{U_{y}}{V_{c}} \tag{7}$$

with  $\theta$  as the angle between the fluid velocity vector and the x-axis.

Now, Equation (4) can be implemented as follows:

$$\frac{\Delta P}{\Delta L}\Big|_{i} = 4.54 \frac{1}{\Delta L_{row}} \left(\frac{\gamma_{A} V_{c} D}{v}\right)^{-0.172} \frac{\rho \gamma_{A}^{2} V_{c}}{2} U_{i} \tag{8}$$

where,  $\Delta L_{row}$  is the row spacing and the subscript i denotes the x or y component.

Equation (1) and (8) are inserted into the momentum equations for the core region as source terms to represent the hydraulic resistance of a matrix of tube bank.

# 3. In-line tube bank experiment

# 3.1 Overview of test rig

As shown in Figure 1, the in-line tube bank consisted of 4 columns wide by 24 rows long tubes enclosed in a rectangular box (0.286m width by 0.2m height). A diameter and pitch of tube is 71.4mm and 33mm, so the pitch to tube diameter ratio (p/d) is 2.16.

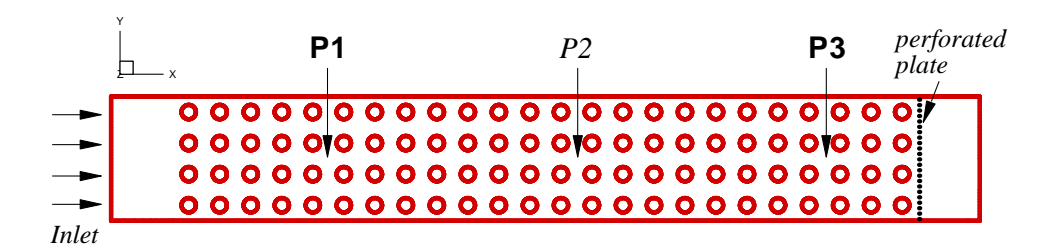


Figure 1 Schematic diagram of in-line tube bank test rig

The inlet consisted of a pyramidal shaped diffuser which was packed with stainless steel mesh between two perforated plates. Flow visualization tests and pressure drop readings confirmed that a uniform flow profile at the entrance of the tube bank was obtained. Another perforated plate was installed at one pitch from the last tube row. This perforated plate minimized exit effects from the flow channel. The first pressure tap was located five pitch lengths into the tube bank. The next two pressure taps were spaced at eight pitch lengths each further into the channel. Porosity, defined as the ratio of fluid-occupied volume to total volume, is about 0.832 for this test rig.

#### 3.2 Numerical method

#### 3.2.1 Grid system and boundary conditions

Figure 2 shows the grid system, which has same dimension as the test rig in Figure 1. As shown Table 1, two types of grid system were used. A variable  $y^+$  denotes the dimensionless distance between the cell centroid and the wall for wall-adjacent cells. Type 2 grid was generated by doubling the number of cells in z-direction (height).

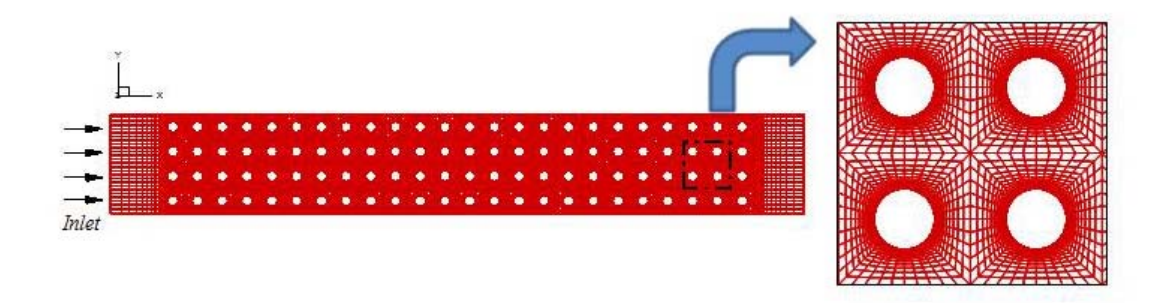


Figure 2 Grid system for in-line tube bank computation

Uniform velocity with the magnitude of 0.054m/s, which corresponds to Reynolds number 2,746, is imposed at inlet boundary. Turbulence intensity at inlet is 4.87% and the turbulence length scale is set to be 11.45mm. The Reynolds stresses at the inlet are derived from the assumption of an isotropic turbulence by using the precalculated turbulence kinetic energy or the turbulence intensity. At the outlet boundary, a zero normal gradient for all flow variables except the pressure is applied. No-slip condition is applied on the solid wall. In FLUENT [3], either wall function or enhanced wall treatment can be used to model the near-wall region. In this study, the prediction with wall function was shown because wall function gave the better prediction results than enhanced wall treatment.

Table 1 Grid system

_	Туре	Cell size	y+		Call tupa	Mall traatmant	
'			Tube wall	Four walls	Cell type	Wall treatment	
	1	879,000	0.4~20	1.5~32.4		Wall function	
	2	1,758,000	0.2~5.3	0.3~7	Hexahedron	or Enhanced	
						wall treatment	

#### 3.2.2 Numerical models

The flow is assumed to be steady, incompressible and turbulent. The first-order accurate upwind differencing for the convection terms of each governing equation is used because this differencing scheme gave the better prediction results and convergence than the second-order accurate upwind differencing in this case. The second-order accuracy is maintained for the viscous terms. The pressure-velocity coupling is handled by the SIMPLE algorithm. The convergence criterion is set to the scaled residuals of  $10^{-5}$  for all relevant variables.

Three different types of the Reynolds-averaged Navier-Stokes (RANS)-based turbulence models, that is, standard k- $\epsilon$ , standard k- $\omega$  and Reynolds Stress Model (RSM), are used to assess the prediction capability of the flow in the in-line tube bank. More detailed descriptions of the numerical models can be found in the FLUENT user's guide [3].

#### 3.2.3 Results

The comparisons of the experimental and calculated pressure drops are summarized in Table 2. The current prediction with real tube geometry gives closer pressure drop values to the measured values between the first and the third pressure taps (P1 and P3) than the MODTURC [1] with the porous medium assumption. Difference between the measurement and the current prediction is below 5.0%. Two equation turbulence models give the better prediction than RSM.

Table 2 Comparison of the magnitude of pressure drop

	Exp.[1]	Porous ass	Present calculation			
	LXP.[1]	MODTURC[1]	CFX-4[9]	k-ε	k-ω	RSM
∆р [Ра]	28.2	30.5	27.6	28.6	28.8	29.6
Error [%]	-	-8.1	2.1	-1.5	-2.1	-5.0

Figure 3 and 4 shows the velocity vector and stream-traces near the position of P1 and P3 measurement. While standard k- $\epsilon$  model and RSM predicted stable and quasi-symmetric flow pattern in the wake region, standard k- $\epsilon$  model showed unstable and asymmetric pattern. According to the calculation of Afgan [10], for p/d = 1.75 symmetrical flow pattern with two recirculation behind the tube was found. Considering that p/d is 2.16 at the present study, it is estimated that both standard k- $\epsilon$  model and RSM give more reasonable prediction than standard k- $\epsilon$  model.

# 4. SPEL experiment

#### 4.1 Overview of test rig

Although a test vessel of the SPEL is not a scaled facility of a real CANDU calandria vessel, it has the typical features of a CANDU reactor, such as a re-circulating jet induced flow, heating of

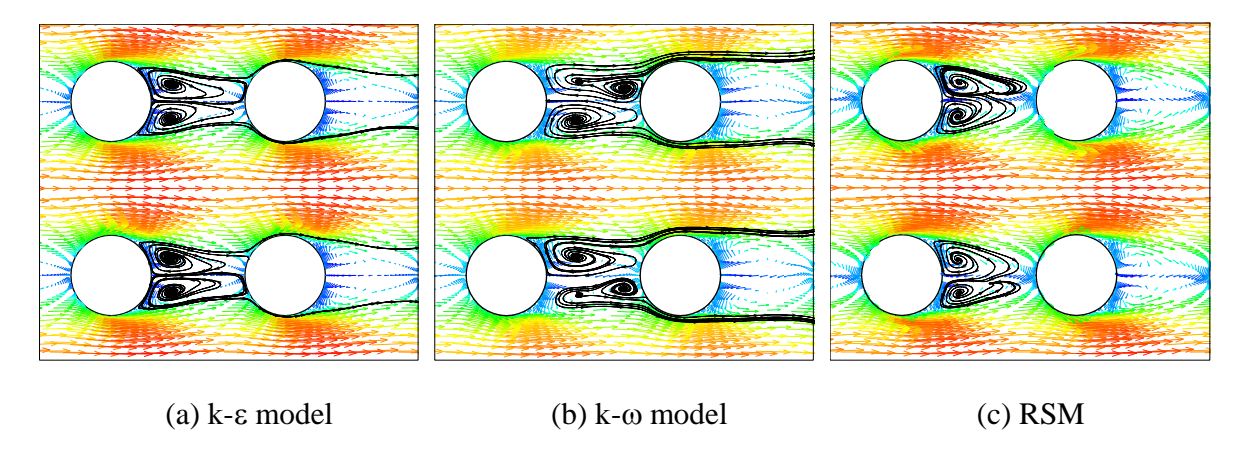


Figure 3 Velocity vector and stream-traces near the position of P1 measurement

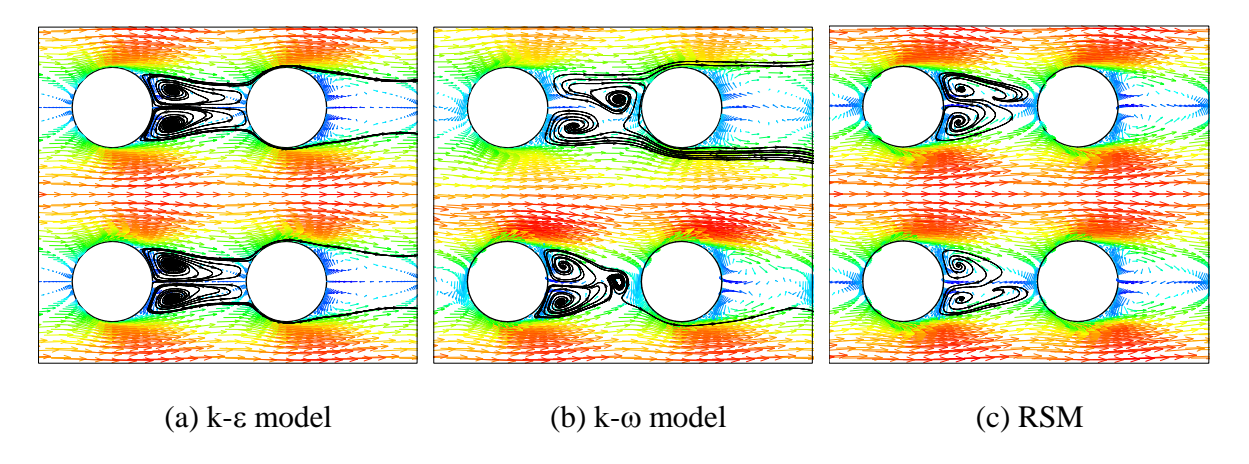
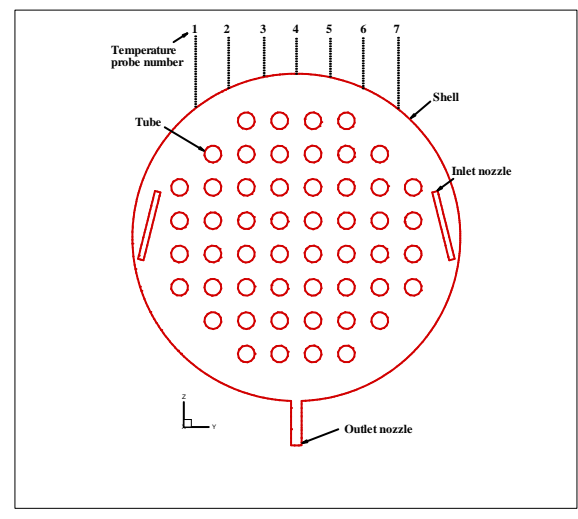
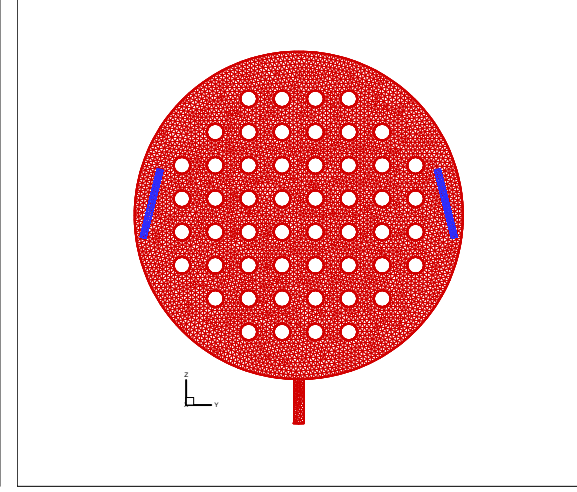


Figure 4 Velocity vector and stream-traces near the position of P3 measurement

the water by volumetric heat generation and a matrix of horizontal tubes parallel to the vessel axis.

A schematic diagram of the test rig is shown in Figure 5(a). The vessel had a transparent acrylic cylindrical shell with 0.737m inner diameter by 0.254m long. A total of 52 copper tubes (0.038m outer diameter by 0.254m long) were arranged on a 0.075m square pitch pattern and installed inside the vessel. Two inlet nozzles were installed along the horizontal centreline at each side of the vessel with an angle of 14° from the vertical direction. The outer part of each nozzle was designed so that it guaranteed a uniform velocity profile at the nozzle exit. One outlet nozzle was installed at the bottom of the vessel. Volumetric heat generation was achieved by electrolytic resistance heating of the dilute sodium chloride solution. The tubes were used as the electrodes. A large amperage alternating current at low potential drop was passed, via these tubes, through the working fluid which acted as a fluid resistor and heat was generated. For the temperature measurement there were seven ports on the top of the cylindrical shell corresponding to the seven vertical lines (1~7) centred between the eight columns of tubes, as shown Figure 5(a).





(a) schematic diagram

(b) grid system (axial mid-plane)

Figure 5 Schematic diagram and grid system of SPEL test rig

#### 4.2 Numerical method

# 4.2.1 Grid system and boundary conditions

Figure 5(b) shows the grid system, which has same dimension as the test rig in Figure 5(a). A total number of cells with unstructured tetrahedral shape are 448,420. A range of  $y^+$  is 0.4~37.1.

Uniform velocity with the magnitude of 0.13m/s, which corresponds to volumetric flow rate of 0.5l/s is imposed at normal to inlet boundary. Inlet fluid temperature is 303.15K. Turbulence intensity at inlet is 3.7% and the turbulence length scale is set to be 12.5mm. The Reynolds stresses at the inlet are derived from the assumption of an isotropic turbulence by using the precalculated turbulence kinetic energy or the turbulence intensity. At the outlet boundary, a zero normal gradient for all flow variables except the pressure is applied. No-slip condition is applied on the solid wall. An adiabatic boundary condition is imposed on the vessel shell. Wall function is used to model the near-wall region. Because the spatial variation of the volumetric heat load for electrolytic resistance heating mode is difficult to evaluate, the volumetric heat load (10kW) is assumed to be uniform inside the test vessel. The volumetric expansion coefficient is required because the Boussinesq model is used to calculate momentum source terms due to buoyancy. In this study, a constant volumetric expansion coefficient of  $5 \times 10^{-4}$  is used.

# 4.2.2 Numerical models

The flow is assumed to be steady, incompressible and turbulent. The first-order accurate upwind differencing for the convection terms of each governing equation is used. The second-order accuracy is maintained for the viscous terms. The pressure-velocity coupling is handled by the

SIMPLEC algorithm, which is recommended for a flow with strong buoyancy effect. The convergence criterion is set to the scaled residuals of  $10^{-3}$  for all relevant variables except  $10^{-6}$  for temperature.

The same turbulence models as used in 3.2.2 are applied. Buoyancy force is modeled using the Boussinesq approximation, which is accurate as long as changes in actual density are small. In this study, while the effects of buoyancy on the generation of turbulence kinetic energy are included, its effects on turbulence dissipation rate are neglected.

# 4.2.3 Results

The fluid flow inside the vessel is very complex due to the interaction between the momentum force generated by the inlet jets and the buoyancy force by heat load to fluid. Test results confirmed that the flow pattern at the test condition of 0.5l/s volumetric flow rate and 10kW heat load was buoyancy dominated flow.

Figure 6 shows the comparisons of experimental and computed temperatures along the port 2 and 4. As shown in Figure 6(a), whereas the current prediction with real tube geometry captures the high temperature region at the upper region of test vessel, previous study with the porous medium assumption [11] underpredicts fluid temperature at the same regions. However, the current study has a tendency to underpredict the fluid temperature at a matrix of tube region. Among three different turbulence models, standard k- $\epsilon$  model gives the best prediction of fluid temperature.

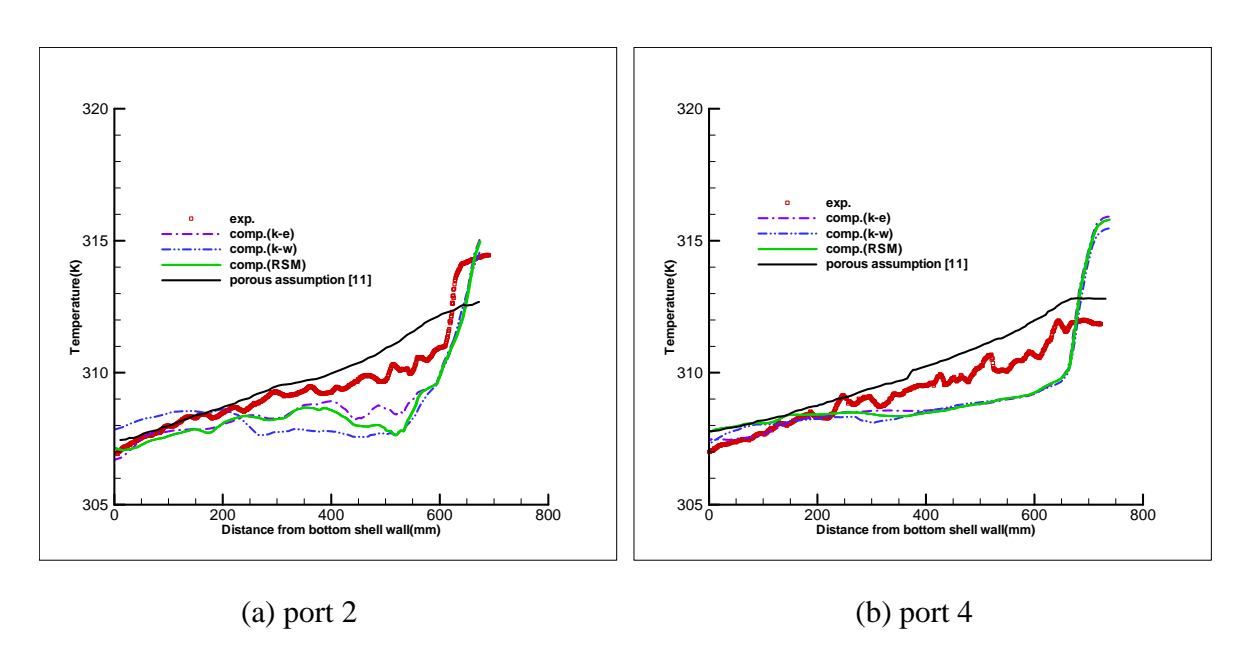


Figure 6 Comparison of experimental and predicted temperatures along the port 2 and 4 (volumetric flow rate: 0.5l/s, heat load: 10kW)

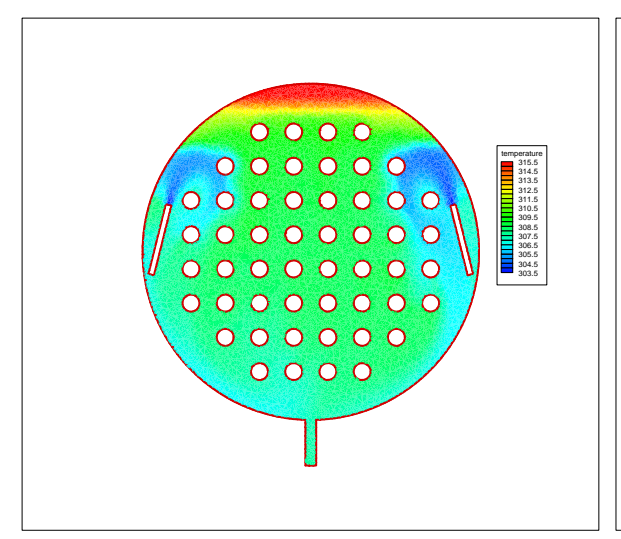
Figure 7 shows the temperature distribution and velocity vector at an axial-mid plane. The fluid flow entering through the inlet nozzle initially travels in the direction of the nozzle. At a small distance from the nozzle the jets circulate and turn its direction towards the vessel shell.

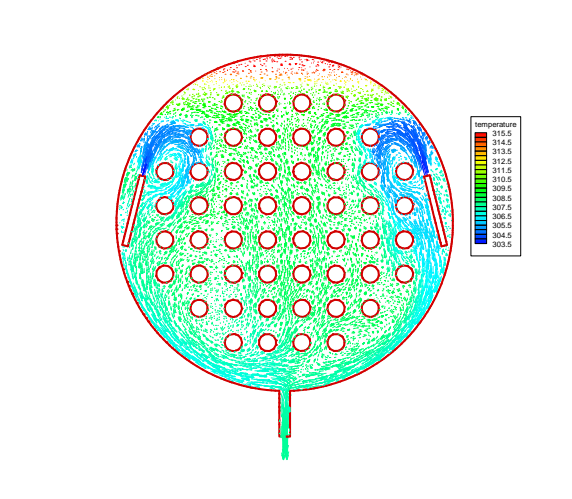
This fluid flow collides with the flow of the opposite side at the bottom of the vessel. Part of the fluid flow exits the vessel from the outlet nozzle and due to the density gradient the remaining fluid flow shows an upward motion in the central region of the vessel. High temperature and low velocity of fluid condition exists at the upper region of the test vessel. Comparing to the test results [2], both k- $\epsilon$  model and RSM show the more reasonable flow and temperature distribution than k- $\omega$  model.

#### 5. Conclusion

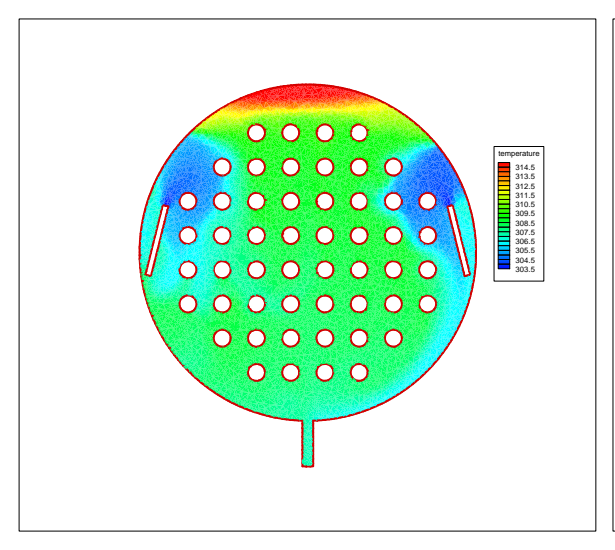
In this paper, sensitivity study on a CFD model for the accurate analysis of moderator fluid flow and heat transfer inside calandria was conducted. Two main items, i.e. porous medium assumption and turbulence model, were considered for in-line tube bank and Sheridan Park Engineering Laboratory (SPEL) experiment. Using the commercial flow solver, FLUENT, the prediction to consider the real geometry of fuel channels was compared to previous results calculated with the porous medium assumption using the isotropic pressure loss model. Also, the prediction performance of various turbulence models was assessed. The major conclusion could be summarized as follows:

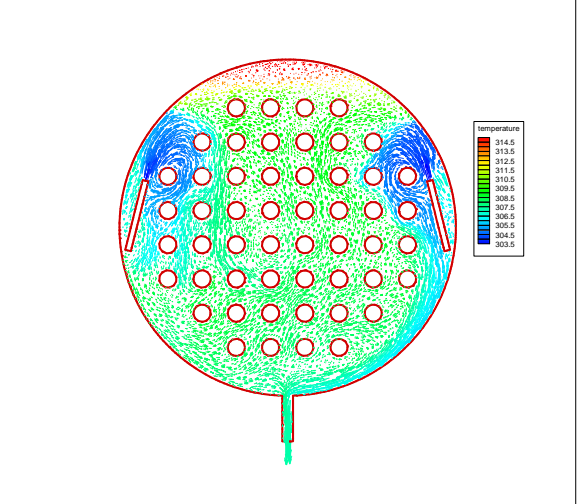
- The prediction to consider the real geometry of fuel channels did not guarantee certainly the better result than the porous medium assumption. This may result from the grid resolution, discretization accuracy and turbulence model.
- Among three different turbulence models, standard k- $\epsilon$  model gave the most reliable prediction.



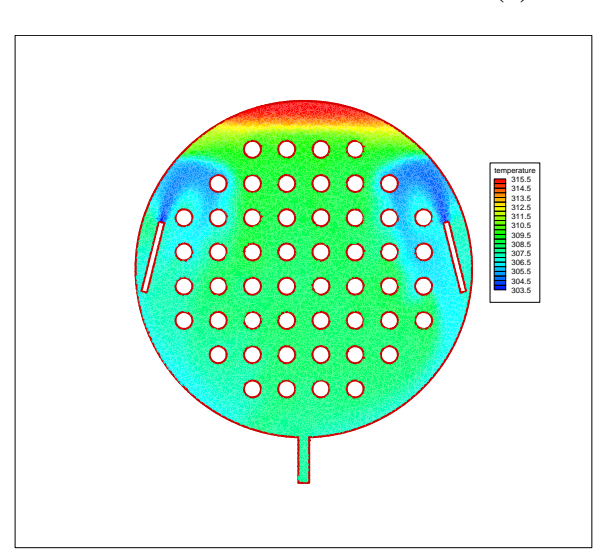


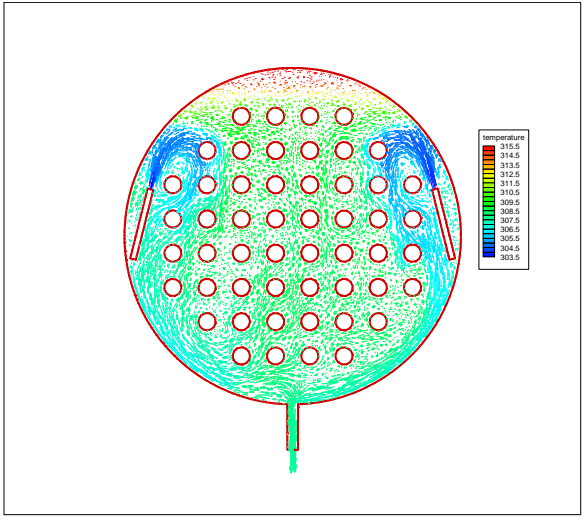
(a) k-ε model (10/12)





(b) k-ω model





(c) RSM

Figure 7 Temperature distribution and velocity vector at an axial-mid plane (volumetric flow rate: 0.51/s, heat load: 10kW)

To enhance the completeness of this study the following items are on-going or will start:

- The isotropic pressure loss model [9] in 3.2.1 will be implemented into the FLUENT via User Define Function (UDF), to compare its prediction performance with real tube geometry case on the same flow solver.
- Prediction performance of another turbulence model, Large Eddy Simulation (LES), will be assessed.

• Whether the porous medium assumption can give the conservative subcooling margin compared to the flow analysis with real calandria tube geometry of CANDU-6 will be checked.

# 6. References

- [1] G.I. Hadaller, R.A. Fortman, J. Szymanski, W.I. Midvidy and D.J. Train, "Frictional pressure drop for staggered and in-line tube banks with large pitch to diameter ratio", 17th Annual Canadian Nuclear Society Conference, Fredericton, New Brunswick, Canada, 1996, June 9-12.
- [2] D. Koroyannakis, R.D. Hepworth and G. Hendrie, "An experimental study of combined natural and forced convection flow in a cylindrical tank", AECL, TDVI-382, 1983.
- [3] "FLUENT user's guide", Version 6.2, FLUENT Inc., 2006.
- (4) "CNSC staff integrated safety assessment of Canadian nuclear power plants for 2009", Canadian Nuclear Safety Commission, INFO-0809, 2010, pp.120.
- [5] W.M. Collins, "Simulation of the SPEL small scale moderator experiments using the general purpose fluid-flow, heat transfer code PHOENICS", TTR-213, 1988, AECL.
- [6] R.G. Huget, J.K. Szymanski and W.I. Midvidy, "Status of physical and numerical modelling of CANDU moderator circulation", 10th Annual Canadian Nuclear Society Conference, Ottawa, Canada, 1989.
- [7] C. Yoon and J.H. Park, "Development of a CFD model for the CANDU-6 moderator analysis using a coupled solver", Annals of Nuclear Energy, Vol. 35, 2008, pp.1041-1049.
- [8] "A review of computer codes MODTURC\_CLAS and PHOENICS", Atomic Energy Control Board, INFO-0624, 1996.
- [9] C. Yoon, B.W. Rhee and B.J. Min, "Development and validation of the 3-D computational fluid dynamics model for CANDU-6 moderator temperature predictions", Nuclear Technology, Vol. 148, 2004, pp.259-267.
- [10] I. Afgan, "Large eddy simulation of flow over cylindrical bodies using unstructured finite volume meshes", Ph.D. thesis, University of Manchester, 2007.
- [11] C. Yoon, B.W. Rhee and B.J. Min, "Validation of a CFD analysis model for predicting CANDU-6 moderator temperature against SPEL experiments", <u>Proceedings of 10th International Conference on Nuclear Engineering</u>, Arlington, Virginia, USA, 2002, April 14-18.